

COVER PAGE

Document downloaded by @DAEL

Sat Nov 28 02:00:45 2026
For personal use

When automatic English translation is provided, only the original document is authentic.
The EAA cannot be held responsible of any translation error

Bibliographical reference

An Extended Model to Predict Reflections from Forests, Jean-Marc Wunderli, Acta Acustica **vol. 98** (Number 2), 2012, pp. 263-278

DOI
https://doi.org/10.3813/AAA.918510

ACTA ACUSTICA UNITED WITH ACUSTICA
Vol. 98 (2012) 263 – 278

DOI 10.3813/AAA.918510

An Extended Model to Predict Reflections from Forests

Jean Marc Wunderli
Empa, Swiss Federal Laboratories for Materials Science and Technology, 8600 Duebendorf, Switzerland.
jean-marc.wunderli@empa.ch

Summary
A model to calculate the sound exposure level due to forest reflections is presented. The model is based on the work published earlier in this journal in which a single tree was solely represented by a vertical cylinder. Comparisons with measurements revealed two weaknesses of the chosen approach. On the one hand it showed that levels could not be predicted correctly at shorter propagation distances. And on the other hand the vertical directivity, i.e., the reflection characteristic with elevation, which was observed in the measurements, could not be reproduced. It turned out that the modeling approach had been chosen too simplistic and that the contributions from the branches cannot be neglected entirely. Therefore the model has been extended to take reflections at the canopy, represented by a number of spheres, into account as well. The model has been implemented in the new Swiss simulation model for railway noise *sonRAIL*. Validations of this implementation with measurements generally show a good agreement with a standard deviation of 2.9 dB(A) up to propagation distances of 500 m. For greater distances the model tends to overestimate the resulting sound exposure level. However the corresponding attenuations at such distances are in the range of 80 dB(A) and therefore the resulting sound exposure is unlikely to yield a relevant contribution to any noise exposure. The deviations up to 500 m can primarily be explained by the distinct properties of the forests involved. In order to further increase the accuracy of predictions specific information about the forest properties would be needed. Mainly the type of trees (hardwood or softwood), the average tree diameter and height as well as the forest density have an influence. However, such information is generally not available and therefore one has to rely on statistical averages, as it was done for this publication. Additionally the accuracy could be increased by applying a more sophisticated propagation calculation with the focus on ground attenuation and meteorological effects. The associated additional computational effort, however, will question an application for noise mapping.

PACS no. 43.20.+g, 43.50.+y

1. Introduction

In 2009 Wunderli and Salomons presented a model to predict the sound reflections from forest [1]. The model was based on the assumption that a single tree can be represented as a vertical cylinder. For the reflection at a cylinder an analytical solution was given based on the theory of scattering of spherical waves. In the publication the model was validated against a set of measurements. Generally a good agreement between calculations and measurements was achieved. Nevertheless the measurements indicated a tendency to overestimate the levels at frequencies above 1 kHz. Therefore in the discussion further validation measurements were recommended and it was also suggested to look into additional aspects such as meteorological influences on forest reflection and vertical directivity.

In the meantime further measurements have been performed and additional data sets have been compared to model calculations. The comparisons revealed two weaknesses of the chosen approach. On the one hand it showed that levels could not be predicted correctly at shorter propagation distances. And on the other hand the vertical directivity, i.e., the reflection characteristic with elevation, which showed in the measurements, could not be reproduced by the chosen model approach with solely a cylinder reflection. It turned out that the modeling approach had been chosen too simplistic and that the contributions from the branches could not be neglected entirely.

In section 2 the extended model is presented and it is shown how the additional contributions from the canopy are represented by reflections of a number of spheres. For the sake of completeness the major equations from [1], which are necessary to follow the complete calculation, are repeated.

The extended forest reflection model has been integrated in the new Swiss simulation model for railway noise *sonRAIL* [2], in combination with a model for reflections from cliffs [3]. *sonRAIL* is designed as an engineering model so quick calculation algorithms are of great im-

Received 3 September 2010,
accepted 26 October 2011.

© S. Hirzel Verlag · EAA

portance. Section 3 yields details about its implementation with the focus on simplifications of the propagation calculation and a reduction of the calculation effort in general. In section 4 a comparison of calculations performed with *sonRAIL* with measurements at four different sites and a total of 60 source-receiver-combinations is shown. The results are discussed in section 5.

2. Extended forest reflection model with additional contributions from the tree canopy - representation of the reflection at a single tree

In [1] an expression for reflectivity R_{cyl}, i.e., the fraction of acoustic energy that is reflected, is given for an infinitely long cylinder as

$$R_{\mathrm{cyl}} = \left[\sum_{m=0}^{\infty} \varepsilon_m \cos(m\phi)(-i)^m H_m^{(1)}(kr)\frac{J_m'(ka)}{H_m^{(1)\prime}(ka)}\right]^2, \quad (1)$$

where ϕ is the scattering angle, i.e. the angle between incoming and reflected sound, r is the shorter distance from the cylinder to the source or the receiver, $k = \omega/c$ is the wave number defined as the ratio of the angular frequency ω and the sound speed c, a is the radius of the cylinder, and $\varepsilon_0 = 1$, $\varepsilon_m = 2$ for $m \geqq 1$. Further, $H_m^{(1)}$ is the Hankel function of the first kind, $H_m^{(1)\prime}$ its derivative, and J_m' the derivative of the Bessel function J. For numerical calculations, the sum in equation (1) can be truncated at $m = 40$ for all frequencies.

The reflection attenuation for a single cylinder $A_{\mathrm{refl,cyl}}$ is calculated according to

$$A_{\mathrm{refl,cyl}} = -10 \cdot \log\left(R_{\mathrm{cyl}}\right). \quad (2)$$

As mentioned in the introduction comparisons with measurements suggest that in certain situations the reflections at branches cannot be neglected. It was therefore decided to modify the forest reflection model by this aspect.

Reflections at the tree canopy are likely to take place mainly at the larger branches. The branches exhibit in comparison to the trunk both a smaller diameter and a smaller length. They are oriented perpendicular to the trunk in all directions. It would be possible to model the branches analogous to the trunk as a number of cylinders with different orientation and size. However the integration over contributions from numerous cylinders with omni-directional orientation will also feature an omni-directional directivity pattern. Hence it was decided to follow an integral approach that does not represent the reflection at single branches but models the tree canopy as a whole by a number of scattering spheres. The spheres could be distributed over the entire canopy. However in comparison with typical propagation distances, it is feasible to locate all spheres at the center of the tree, i.e., at half of the tree height. This allows for reducing the calculation effort substantially as only the reflection at a single sphere has to be calculated and the contributions from additional spheres can be considered with a simple multiplication factor.

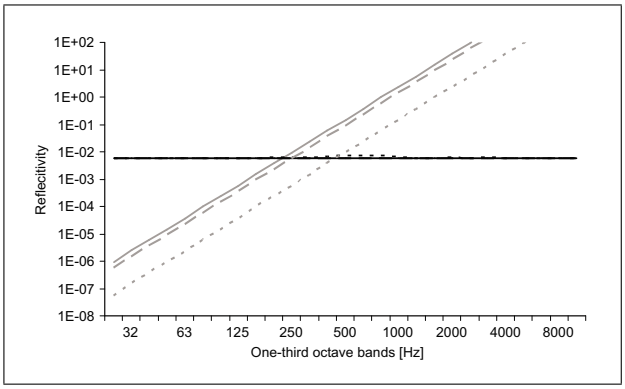


Figure 1. Reflectivity of a sphere with radius 15 cm. The solution valid for low frequencies is given in gray and the one for high frequencies in black. For both solutions scattering angles of 0, 45 und 90° are shown as solid, dashed and dotted lines respectively.

The radius of the sphere is set to 15 cm. Compared to the typical dimensions of the branches, this radius seems rather big. It was chosen as a consequence of the fact that a cylinder reflects more effectively at low frequencies than a sphere of the same diameter. This loss of reflection by the change from a cylinder reflection to the reflection of a sphere is thereby compensated accordingly.

The number of spheres that are placed in the tree canopy defines the strength of the reflection. In comparison with the measurement data that will be presented in section 4 a representative value of 250 was derived for a single tree.

Based on a solution for rigid spheres by Morse and Ingard [4] the reflectivity of a sphere R_{sph} can be given as

$$R_{\mathrm{sph}} = \min\begin{cases} \dfrac{k^4 a^6}{9}\left[1 - 3\cos(\pi - \phi)\right]^2 \\ \dfrac{a^2}{4}\left[1 + \cot^2(\pi - \phi/2)\right. \\ \qquad \left.\cdot J_1^2(ka\sin(\pi - \phi))\right] \end{cases} \quad (3)$$

where ϕ is the scattering angle, i.e., the angle between incoming and reflected sound, k is the wave number, a is the radius of the sphere and J_1 is the Bessel function of the first order. The solutions according to [4] were derived based on the assumption that $ka \ll 1$ (valid for low frequencies) and $ka \gg 1$ (valid for high frequencies) respectively. Figure 1 shows examples of ρ_{sph} for both solutions for scattering angles of 0, 45 and 90°. For each scattering angle the frequency is derived at which both solutions yield the same result. Below this frequency the solution for low frequencies and above the solution for high frequencies is used.

The reflection attenuation for the spheres of a single tree $A_{\mathrm{refl,sph}}$ is calculated according to equation (4) with N_{sph} as the number of spheres, set to 250.

$$A_{\mathrm{refl,sph}} = -10 \cdot \log\left(N_{\mathrm{sph}} \cdot R_{\mathrm{sph}}\right). \quad (4)$$

2.1. Propagation calculation for the contributions of trunk and branches of a single tree

The sound level of the reflection yielded by the trunk of a single tree in a forest is calculated according to equation (5) where L_W is the sound power level of the source and the remaining terms are attenuations due to geometrical divergence of the sound field, atmospheric absorption, foliage, the reflection at the trunk and the excess attenuation, respectively.

$$L_{\mathrm{cyl}} = L_W - A_{\mathrm{geo,cyl}} - A_{\mathrm{atm}} - A_{\mathrm{fol}} - A_{\mathrm{refl,cyl}} - A_{\mathrm{ex}}. \quad (5)$$

In equation (6) the corresponding expression for the reflection at the branches is given.

$$L_{\mathrm{sph}} = L_W - A_{\mathrm{geo,sph}} - A_{\mathrm{atm}} - A_{\mathrm{fol}} - A_{\mathrm{refl,sph}} - A_{\mathrm{ex}}. \quad (6)$$

Geometrical divergence for the cylinder is calculated with $A_{\mathrm{geo,cyl}} = 10 \cdot \log[4\pi(r_s + r_r)^2]$ with r_s the distance from the source to the cylinder and r_r the distance from the cylinder to the receiver. Geometrical divergence for the spheres is calculated with $A_{\mathrm{geo,sph}} = 10 \cdot \log[4\pi(r_s \cdot r_r)^2]$ with r_s and r_r defined correspondingly. A_{atm} shall be calculated according to ISO 9613-1 [5] and A_{fol} according to ISO 9613-2 [6]. The excess attenuation A_{ex} comprises additional propagation effects such as ground attenuation, shielding effects as well as meteorological influences on sound propagation. It is recommended not to do a propagation calculation for each tree but to perform the calculation as proposed in [1] by assuming a rigid, reflecting wall along the forest edge. The propagation model for that task has to be sufficiently sophisticated to be able to take these effects into account. (Recommended are ray tracing models or PE-models [7], [8].)

The contributions from the trunk and the branches are summed up energetically according to equation (7) to derive the sound exposure level produced by the reflection at a single tree L_{Tree}. However, additionally a frequency dependent weighting function is applied for the contribution of the trunk w_{cyl}, which was derived in comparison with measurements. The contribution from the trunk is fully accounted up to a frequency of 250 Hz. From 250 Hz to 1000 Hz w_{cyl} is set to 0.5. Above 1000 Hz w_{cyl} is halved again, amounting to a factor of 0.25.

$$L_{\mathrm{Tree}} = 10 \cdot \log\left(\left[10^{-w_{\mathrm{cyl}} \cdot L_{\mathrm{cyl}}/10} + 10^{-L_{\mathrm{sph}}/10}\right] \right). \quad (7)$$

The reduction of the reflection efficiency of the cylinder can be explained by the presence of the branches. At higher frequencies the sound wave is influenced on its way forth and back to the trunk by the branches and experiences a distortion of the phase relation within the reflected wave. At lower frequencies, as the branches are smaller than the trunk itself, this distortion is less pronounced and therefore the reflection at the cylinder primarily takes place undisturbed.

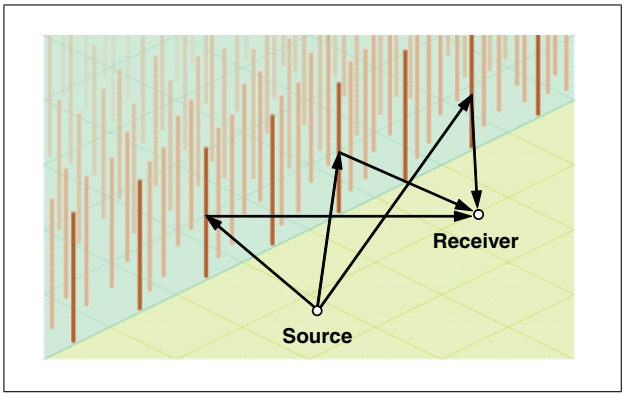


Figure 2. Calculation scheme for forest reflections where a propagation calculation is only performed for representative cylinders at the forest edge.

3. Implementation in the engineering sound propagation model of *sonRAIL*

The calculation procedure presented in section 2 for the reflection at a single tree can directly be applied to entire forests by modeling each tree individually. However as forests generally exhibit thousands of trees the corresponding computational times tend to get very large. In order to do noise mapping it is therefore necessary to introduce several simplifications and accelerations. In this section the implementation of the forest reflection model in the engineering sound propagation model of *sonRAIL* [2] is shown.

3.1. Focus on representative trees

The reflection of an entire forest is represented by superposing the contributions of all trees. On the one hand the trees in a typical forest are not positioned in a regular grid but show within certain limits an arbitrary distribution. On the other hand the spacing between the trees is great compared to the wavelengths of interest. Hence it can be followed that the summation of the reflected signals of the individual trees can be carried out incoherently. This conclusion allows important simplifications and accelerations of the calculation procedure. Instead of calculating the reflection of every tree in a forest in proper phase it is feasible only to do propagation calculations for a few representative cylinders and to account for the contributions of other trees by simple multiplications.

In *sonRAIL* forests are defined by closed polygons. The forest edge is divided into segments where only one tree on the forest edge is calculated per segment (see Figure 2). In order to determine the contribution of the trees from the depth of the forest an empirical correction is used, that was already presented in [1]. The number of trees per segment N in this correction is derived according to equation (8).

$$N = \mathrm{Min}\left[\frac{d_{\mathrm{seg}}}{d_{\mathrm{for}}} \frac{1}{u[x,y] + v\ln(\lambda)}, \frac{d_{\mathrm{seg}}}{2a}\right], \quad (8)$$

where d_{seg} is the length of the segment and d_{for} is the average distance between trees in a forest. Based on statis-

tical data of forests in Switzerland given in [1] d_{for} is set to a default value of 4.5 m. (From the same statistics a representative cylinder diameter of 27 cm and a typical tree height of 20 m were derived.) The expression in the denominator depends on geometry and frequency. It was derived by comparing simulations where all trees in a forest were calculated with situation where only the trees at the forest edge were taken into account. Parameter v accounts for the frequency dependency and was determined as -0.03. $u[x, y]$ is given in equation (9).

$$u[x,y] = g + h \cdot f_x + i \cdot f_y + j \cdot f_x f_y + k \cdot f_x^2 f_y + l \cdot f_x f_y^2 + m \cdot f_x^2 f_y^2, \quad (9)$$

with $x = \min(r_r, r_s)$, $y = (r_r + r_s)^2$, $x_{\mathrm{Min}} = 7.5$, $x_{\mathrm{Max}} = 400$, $y_{\mathrm{Min}} = (7.5+50)^2$, $y_{\mathrm{Max}} = (500+400)^2$,

$$f_x = \frac{\ln[x/x_{\mathrm{Min}}]}{\ln[x_{\mathrm{Max}}/x_{\mathrm{Min}}]}, \quad f_y = \frac{\ln[y/y_{\mathrm{Min}}]}{\ln[y_{\mathrm{Max}}/y_{\mathrm{Min}}]}.$$

The free parameters were optimized to yield a least-square-fit resulting in the following values: $g = 0.484$, $h = -0.387$, $i = -0.203$, $j = -0.713$, $k = 1.313$, $l = 0.814$, $m = -1.171$.

With the second criterion in equation (8) it is guaranteed that the number of trees does not exceed the case of a closed wall, i.e., a situation with no space between cylinders. In agreement with equation (1) a is the cylinder radius.

The number N of trees per segment was derived only taking cylinder reflections into account. As geometrical divergence is different for a cylinder reflection than for the scattering at a sphere a comparable analysis for the reflection at the branches would yield different results. Nevertheless it was decided for *sonRAIL* to rely on the same expression for the cylinder reflection as well as for the spherical reflection. When analyzing the behavior of equation (8) it turns out that sound penetrates deep into the forest under two conditions: if frequencies are low and if source and receiver are far away from the forest edge. Exactly under such conditions the contributions from the spheres are likely to be of less importance, as a consequence of the geometrical spreading and the frequency characteristics of the reflectivity. In the opposite case with short propagation distances and at higher frequencies the penetration depth is limited to a few meters and the difference between cylinder reflections and reflections at the spheres becomes small.

In situations over level terrain it is sufficient to calculate forest reflections solely on the basis of reflectors placed along the forest edge. In narrow valleys it may occur that source and receiver are situated on one slope of the valley and that the other slope is entirely covered by a forest. In these rather seldom situations reflections from the forest roof have to be taken into account as well. Therefore additional representative trees are incorporated in *sonRAIL* in the middle of the forest. The empirical correction according to equation (8) was derived on the basis of simulations with a forest of 100 m depth. Therefore these additional trees are placed on a horizontal grid with a spacing of 100 m.

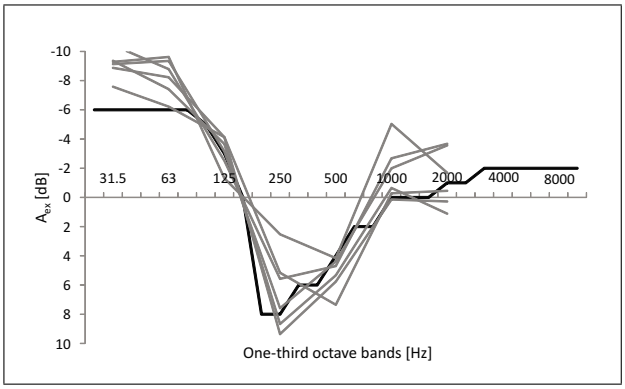


Figure 3. Standardized excess attenuation spectrum A_{ex} for forest reflections for the propagation path source-reflector-receiver in black. Additionally the excess attenuations used in [1] are depicted in grey.

The decision not to calculate every single tree but to focus on a few representative ones is a major key to get the forest reflection model suitable for engineering sound propagation models. Within *sonRAIL* additional measures were taken to speed up the individual propagation calculations.

The calculation of the reflectivities according to equations (1) and (3) is comparably time consuming. Therefore, as proposed in [1], one-third octave band spectra of R_{cyl} and R_{sph} are stored in a look-up table for specific scattering angles and a reference distance. Reflections at horizontal scattering angles of more than 135° are being ignored.

3.2. Simplification of the propagation calculation

Looking at the propagation calculation itself, the determination of the excess attenuation A_{ex} is the laborious and time consuming task. As it has to be performed for each source and receiver combination and for each segment of each forest edge, calculation times tend to explode when doing noise mapping. The resulting sound exposure level on the other hand is averaged over many propagation paths. The corresponding average excess attenuation therefore exhibits a docile bearing with similar characteristics for typical geometries. Therefore it was decided for *sonRAIL* to omit meteorological effects and to use a look-up table with an idealized ground attenuation spectrum. This standardized excess attenuation spectrum as depicted in Figure 3 has been derived in comparison with the PE-calculations presented in [1], reproducing a rather broad ground effect dip around 250 Hz. However the idealized spectrum deviates from the PE-calculations at low frequencies, where the ground attenuation is limited to a pressure doubling. As will be discussed in the following section 3.3 the additional increase in the resulting sound exposure level cannot be attributed to the reflection at the ground but is a consequence of the limited reflector height and shall be treated separately. Towards higher frequencies, the standardized excess attenuation approaches -2, i.e., a slight increase of the result-

ing sound exposure level typical for an energetic superposition of direct and reflected sound over a ground with moderate flow resistivity. The raising of the excess attenuation around 1 kHz which shows in three of the six spectra based on PE-calculations according to Figure 3 is not represented in the standardized excess attenuation. The interference pattern at higher frequencies varies significantly in dependence of geometry and it was decided to rely on a spectrum with a monotonous transition instead. The standardized excess attenuation spectrum is assumed to be representative for propagation situations over grassland with only a few meters height above ground and propagation distances of a few hundred meters. Despite the fact that the ground impedance in forests is typically smaller than over grassland [9], [10], [11] the assumption of a ground with moderate flow resistivity seems valid as the simulations discussed in section 3.1 clearly showed that the reflections are dominated by the first rows of trees. Consequently the reflection at the ground is predominantly taking place outside of the forest.

Likewise barriers are also treated in a simplified way in the implementation of the forest reflection model in *sonRAIL*. Instead of calculating shielding effects, only a visibility check is applied. If the line of sight is either blocked from the source to the reflector or from the reflector to the receiver it is assumed that the contribution of the corresponding segment of the forest edge can be neglected and accordingly no reflection calculation is performed.

3.3. Consideration of the limited reflector height

In Figure 4 a simulation of the reflection at a rigid circular plate is depicted to illustrate the influence of the reflector size. When starting with a small reflector, an increase of the reflector radius leads to an increase of the reflected sound pressure. The reflection reaches a maximum when the additional path length via the reflector edge equals half a wavelength λ relative to the path via the reflector center, i.e., when the reflector covers one Fresnel-zone [12]. At this point the reflected sound pressure yields twice the magnitude compared to a reflector with unlimited size. When the reflector size is further increased destructive interferences cause a reduction of the resulting sound pressure signal. Further on a typical interference pattern is evolving with constructive and destructive interferences that follow each other in shorter intervals, approximating the case of a reflector with unlimited size.

Typically when calculating reflections in engineering models only a reduction of the reflection is taken into account as a consequence of a too small reflector size. For a reflector dimension that exceeds the area of the first half Fresnel-zone, a full reflection as for a reflector of unlimited size is assumed. However when looking at Figure 4 and considering the typical tree heights of around 20 m it becomes obvious that the first overshoot with a level increase of up to 6 dB relative to the unlimited reflector is taking place at distances and frequencies that are within the scope of the model. Therefore it was decided to also

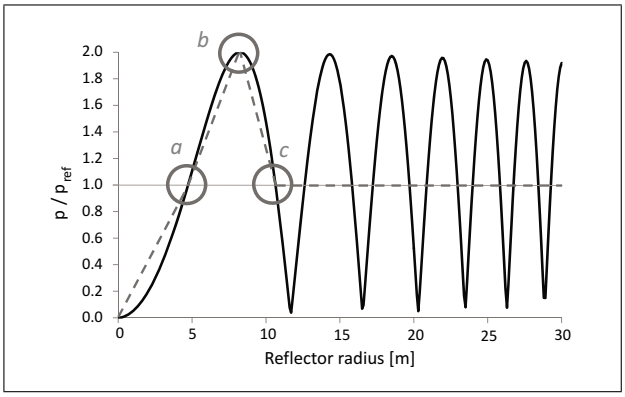


Figure 4. Predicted dependence of the reflected sound pressure at a circular reflector on the reflector radius, normalized to the reflection p_{ref} of a reflector with unlimited size. The simulation has been performed for 250 Hz and with source and receiver centered over the reflector in 100 m distance. Additional sound paths relative to the direct path of $1/4\lambda$, $1/2\lambda$ and $3/4\lambda$, i.e., 0.5, 1.0 and 1.5 Fresnel zones, are labeled and marked with circles. The dashed line in grey shows the Fresnel factor Π that is used in the engineering model to represent the influence of the reflector size.

consider this first overshoot when taking the limited reflector height into account. It was also decided not to represent interference pattern that follow later on as the averaging process flattens quicker under practical conditions than shown in Figure 4, on the one hand as contributions of many trunks are superimposed and on the other hand as third-octave bands instead of single frequencies are dealt with.

In order to derive a correction to account for the limited reflector height, the dimensions of the Fresnel-zones *a*, *b* and *c* as shown in Figure 4 are determined in the vertical plane of the reflecting cylinder and are compared with the length of the cylinder that is covered by these Fresnel-zones. Therewith by interpolation a Fresnel factor Π is derived according to equation (10) which reproduces the influence of the reflector size as given in Figure 4 in a simplified way. The analysis, how many Fresnel-zones are actually covered by the reflector has to be performed for each one-third octave band and also to both sides of the reflection point separately, i.e., the intersection point of the line between receiver and mirrored source with the straight line through the cylinder as shown in Figure 5. The two corrections for both sides of the reflection point are averaged (equation (11)). The Fresnel factor Π is incorporated in a modified expression of the reflection attenuation according to equation (12).

$$\Pi_n(\lambda) = \begin{cases} \dfrac{l_{\mathrm{cyl,n}}}{l_{\mathrm{Fa,n}}(\lambda)} & \text{for } l_{\mathrm{Fa,n}}(\lambda) \geq l_{\mathrm{cyl,n}}, \\ 1 + \dfrac{l_{\mathrm{cyl,n}} - l_{\mathrm{Fa,n}}(\lambda)}{l_{\mathrm{Fb,n}}(\lambda) - l_{\mathrm{Fa,n}}(\lambda)} & \text{for } l_{\mathrm{Fb,n}}(\lambda) \geq l_{\mathrm{cyl,n}} > l_{\mathrm{Fa,n}}(\lambda), \\ 2 - \dfrac{l_{\mathrm{cyl,n}} - l_{\mathrm{Fb,n}}(\lambda)}{l_{\mathrm{Fc,n}}(\lambda) - l_{\mathrm{Fb,n}}(\lambda)} & \text{for } l_{\mathrm{Fc,n}}(\lambda) \geq l_{\mathrm{cyl,n}} > l_{\mathrm{Fb,n}}(\lambda), \\ 1 & \text{for } l_{\mathrm{cyl,n}} > l_{\mathrm{Fc,n}}(\lambda), \end{cases} \quad (10)$$

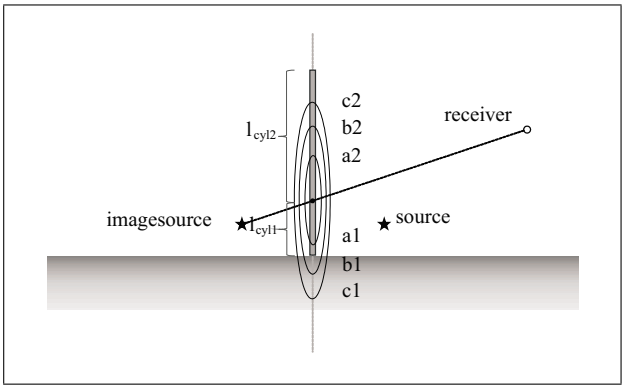


Figure 5. Visualization of the parameters needed to derive the Fresnel factor Π according to equation (10). $l_{cyl,1}$ and $l_{cyl,2}$ are the lengths of the reflecting cylinder below and above the reflection point. *a*, *b* and *c* denote the Fresnel zones corresponding to additional path lengths of $1/4\lambda$, $1/2\lambda$ and $3/4\lambda$ as shown in Figure 4.

$$\Pi(\lambda) = \frac{\Pi_1(\lambda) + \Pi_2(\lambda)}{2}, \tag{11}$$

$$A_{refl,cyl} = -10 \cdot \log\left(\Pi^2 \cdot R_{cyl}\right). \tag{12}$$

4. Model validation

In this section forest reflection measurements at four sites in Switzerland are presented and compared with calculations. Two sites, located close to 'Thun' and 'Dinhard', featured flat terrain and the other two sites in 'Eglisau' and 'Wald' were located at valley slopes. Generally the measurements were performed along straight forest edges of lengths that clearly exceeded the maximum distance of sources or receivers from the forest edge. In 'Dinhard', 'Eglisau' and 'Wald' propagation distances were rather short such that meteorological influences can be excluded. In 'Thun' measurements were performed during several campaigns and different weather conditions with receiver positions up to 300 m and source positions up to 500 m away from the forest edge. The forests in 'Thun' and 'Eglisau' primarily exhibited hardwood, those in 'Dinhard' and 'Wald' primarily softwood.

4.1. Description of the measurements

In 'Thun' measurements were performed at five different days with three different source positions and eight different receiver locations. Table I yields time and date of the experiments as well as the coordinates of the source and microphone positions. The microphones were placed at a height of 4 m above terrain. As sound sources 5 to 10 charges of either 200 g TNT (Source S1) or 50 g TNT_{eq} (explosive material: Plastit, Source S2) were ignited on a steel plate on the ground.

The meteorological conditions were either recorded with a conventional meteorological station, type Reinhardt MWS 9, at a height of 10 m or with a three-dimensional ultrasound-anemometer, type Metek USA1, at a height of 3 or 4 m. During the night time measurements of 2007 additionally temperature measurements were performed at 1, 3 and 10 m height.

The measurements in 2002 were performed at three different days. Day 1 was a warm summer day with only minor cloudiness and moderate winds between 0 and 2 m/s. The major wind direction was 26°, corresponding to downwind conditions for the direct sound. The second day exhibited a clear sky with choppy winds between 2 and 6 m/s. The wind was mainly blowing from 328°, also representing a downwind condition. The third set of measurements took place early in the morning in October. At the beginning it was calm and a nightly inversion still seemed to be present. Later on a wind of 2 to 4 m/s came up with a main direction of 136°, representing upwind conditions for direct sound.

Table I. Measurement geometry of the measurements performed in 'Thun'. (Note: The center of the coordinate system is placed at the edge of the forest with at least 250 m of forest to both sides. *X* denotes the distance to the forest edge, *Y* denotes the distance parallel to it). Source type S1: 200 g TNT, S2: 50 g Plastit. Receiver types R*n*, $n = 1 \ldots 6$ All values in meters.

ID	Date, Time	Source	X	Y	Receiver	X	Y
2a	2002-06-27 9:15–10:45	S1	505	0	R1	173	0
					R2	79	0
2b	2002-07-04 8:30–11:00	S1	505	0	R1	173	0
					R2	79	0
2c	2002-10-31 8:30–11:00	S1	505	0	R2	79	0
					R3	29	0
3a	2003-09-05 10:45–11:15	S2	47	0	R1	97	0
					R2	197	0
					R3	296	0
					R5	100	150
					R6	100	250
4a	2003-09-05 11:20–11:50	S2	147	0	R1	97	0
					R2	197	0
					R3	296	0
					R5	100	150
					R6	100	250
3b	2007-11-06 20:00–20:50	S2	47	0	R1	97	0
					R2	197	0
					R3	296	0
					R4	100	75
					R5	100	150
4b	2007-11-06 21:00–21:40	S2	147	0	R1	97	0
					R2	197	0
					R3	296	0
					R4	100	75
					R5	100	150

The measurement campaign in 2003 was performed on a sunny September day with wind speeds between 1 and 2 m/s coming from an average direction of 133°.

The experiment of 2003 was repeated in 2007. However this time at nighttime with almost no wind and a clear sky. This measurement situation had been chosen on purpose to be able to measure a nightly inversion in order to get favorable propagation conditions in all directions. The analysis of the temperature measurements approved, that the aspired conditions were present.

The measurements of the years 2002 and 2003 had been performed with sound level meters of the type Brüel & Kjaer 2230. The signals had been recorded on DAT audio recorders of the type Sony TCD D-10 PRO. Direct sound and reflections were separated by temporal windowing. A spectral analysis was performed for octave bands of 31.5 Hz to 4 kHz. In the measurements of 2007 sound level meters of the type Brüel & Kjaer 2238 were used together with portable audio recorders of the type Sound Device 702T and 744T respectively. Again direct sound and reflections were separated by temporal windowing. This time a spectral analysis was performed for one-third octave bands from 10 Hz to 10 kHz.

The results of 'Thun' were completed with additional data of forest reflections over level ground that had been collected 1993 during another project. As indicated in Table II these measurements in 'Dinhard' had been performed much closer to the forest edge. As sound source a pistol of 9 mm calibre was operated using blind cartridges (Source S3). Two times ten rounds were shot, holding the pistol once straight up and once horizontal, parallel to the forest edge. No weather data was recorded, due to the short propagation distances. The measurement equipment and the analysis of the recorded data were the same as in 2002 and 2003. Yet as the pistol did not yield enough sound energy at low frequencies an analysis of the octave bands of 63 Hz or below was not possible in most cases.

Measurements over sloped terrain were performed 2009 in 'Eglisau' with an average incline of 27 % and in 'Wald' with an average incline of 50 %. In both situations different source positions and four microphones on a stand of 12 m height were used in order to get a wide range of vertical reflection angles. Figures 6 and 7 give a side view of the situations and Table III yields the corresponding geometries. As sound source a signal pistole of the type WBAG 94 was used (Source S4). At each source position five shots were fired off. The signals were recorded with the same measurement equipment as used 2007 in 'Thun'. One-third octave bands were analyzed from 50 Hz to 10 kHz. Again, as a consequence of the short propagation distances, no meteorological data was recorded. As an example Figure 8 shows a level vs. time diagram for one situation measured in 'Eglisau'.

4.2. Comparison of calculation results with measurements

The calculations were performed for one-third octave bands from 50 to 5000 Hz with standardized parameters

Table II. Geometry of the measurements performed in 'Dinhard'. (Note: The center of the coordinate system is placed at the edge of the forest with at least 100 m forest to both sides. *X* denotes the distance to the forest edge, *H* denotes the height above terrain.)

Receiver	X	H	Source	X	H
R1	5 m	4.0 m	S3	50 m	1.9 m
R2	15 m	4.0 m			
R3	30 m	4.0 m			

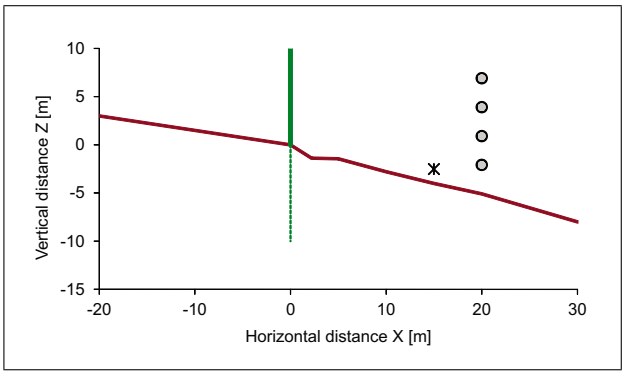


Figure 6. Side view of measurement geometry 5a in 'Eglisau'. At a horizontal distance of 0 m the forest edged is indicated. The cross denotes the position of the source and the circles the positions of the four microphones in heights of 3, 6, 9 and 12 m above ground.

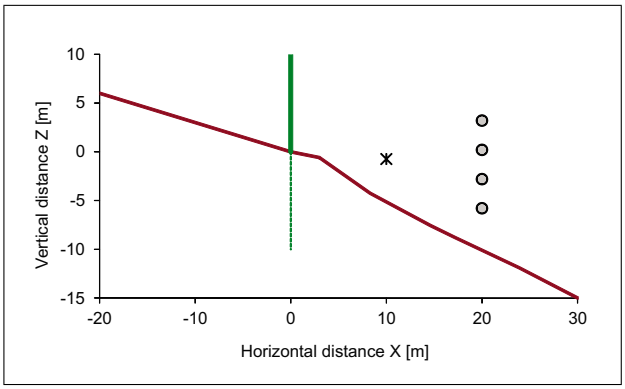


Figure 7. Side view of measurement geometry 6a in 'Wald'. At a horizontal distance of 0 m the forest edged is indicated. The cross denotes the position of the source and the circles the positions of the four microphones in heights of 3, 6, 9 and 12 m above ground.

for the forest height (20 m), the forest density (5 trees per 100 m^2) and the average diameter of the tree trunks (27 cm) according to the statistical analysis of forests in Switzerland given in [1]. Air absorption was calculated with standardized values, i.e., a temperature of 8°C and a humidity of 76%.

The sound energy level of the impulse sources, that were used for calculation, are given in Figure 9. The emission data of the explosions was calculated as Weber-spectra (see ISO 17201-2 [13] and ISO 13474 [14]). The effective source heights of the explosions were derived according

Table III. Geometry of the measurements performed in 'Eglisau' and 'Wald'. The position of the lowest microphone R1 is indicated. Three additional microphones R2 to R4 were placed each 3 m higher. (Note: The center of the coordinate system is placed at the edge of the forest with at least 100 m forest to both sides. *X* denotes the distance to the forest edge, *Z* denotes the height relative to the root point of the forest edge.)

Eglisau	Source		Receiver	
ID	X	Z	X	Z
5a	15 m	-2.52 m	20 m	-2.10 m
5b	30 m	-6.50 m	20 m	-2.10 m
5c	30 m	-6.50 m	20 m	-3.60 m
5d	15 m	-2.52 m	20 m	-3.60 m
Wald	Source		Receiver	
ID	X	Z	X	Z
6a	10 m	-0.75 m	20 m	-5.80 m
6b	15 m	-4.05 m	20 m	-5.80 m
6c	15 m	-6.05 m	20 m	-5.80 m
6d	25 m	-10.40 m	20 m	-5.80 m
6e	30 m	-13.50 m	20 m	-5.80 m

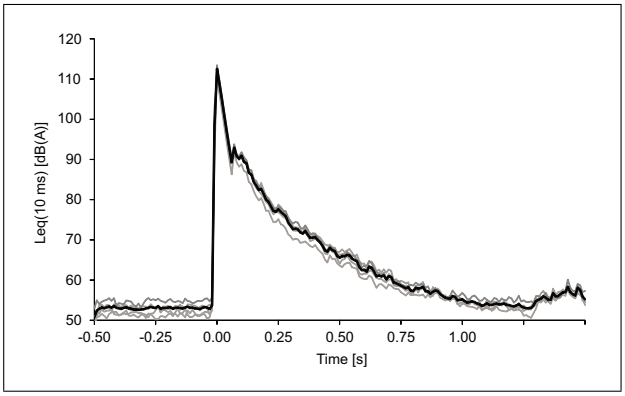


Figure 8. A-weighted level vs. time diagram for geometry 5a and the lowest microphone of the situation in 'Eglisau'. The signals in gray show 5 single shots and the signal in black the average over those 5 shots. Reflections have been analyzed between 0.07 and 1.2 s.

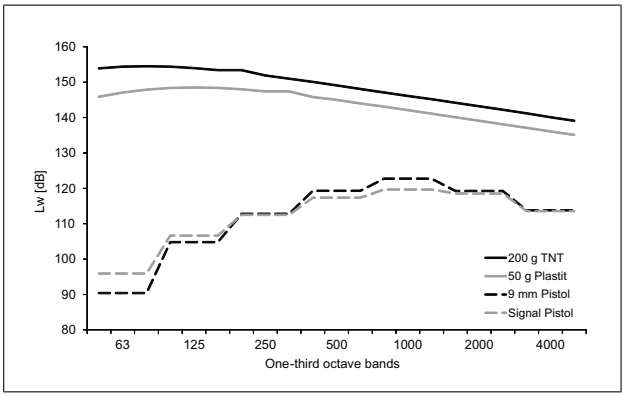


Figure 9. Sound energy spectra of the impulse sound sources that were used during the measurement campaigns.

to [15] equaling 1.15 m for the charges of 200 g TNT and 0.70 m above ground for the charges of 50 g TNT_{eq}.

The measured sound exposure levels were averaged energetically over all events of a distinct situation. The sound attenuations are calculated as differences from the emission data given in Figure 9.

In the Figures 10 to 24 one-third octave band spectra from 50 Hz to 5 kHz are depicted for all situations. The data is organized chronologically. Apart from the combined contributions from cylinders and spheres also the sound exposure levels solely produced by the cylinders are shown. When comparing the contributions from cylinders and spheres it becomes obvious that the spherical reflections are dominant at smaller propagation distances and tend to become less important the further away source and receiver are from the forest edge.

Figures 18 to 24 show the experiments that were performed to gather information on the vertical directivity of forest reflections. Generally a slight decrease in the measured sound exposure level can be seen, the further the reflection path deviates from the horizontal plane. This effect is well represented by the calculations. Peculiar is how the contribution from the cylinders decreases and even vanishes for source and receiver points well below the level of the trees. Accordingly the vertical directivity pattern is primarily produced by changing reflections at the trunk. As the contributions from the trunk are more important for the overall sound exposure level at greater distances, it can be concluded that the directivity pattern of forest reflections is pronounced at greater distances.

Figure 25 yields a compilation of the resulting frequencies of occurrence of deviations between measured and calculated attenuations. The results of this comparison, which is performed in one-third octave bands, is subsequently discussed for each situation individually.

The experiment in 'Dinhard' was performed with source as well as receiver positions at a short distance from the forest edge. As can be seen in Figure 10 the accordance between measured and calculated data is fairly good with only a slight underestimation of the resulting sound exposure levels at frequencies below 250 Hz, which might be ascribed to influences from background noise. 75% of all one-third octave band values exhibit deviations smaller than ± 4.5 dB, i.e., the sum of the classes of -3, 0 and 3 dB deviation in Figure 25.

In Figure 11 the experiments in 'Thun' of the year 2002 are depicted. Here the propagation distances were far greater with a source position over 500 m away from the forest edge. The comparison with measurements shows a systematic overestimation by the model. In total the calculated one-third octave band sound exposure level exceeded the measurements in 75% of all cases. This result is not satisfactory, especially as only 29% of all one-third octave band deviations lie within ± 4.5 dB. Especially great are the deviations in a frequency range around 250 Hz in comparison with the data of the first execution of measurements.

The experiments in 'Thun' in 2003 and 2007 were performed with source and receiver locations in distances

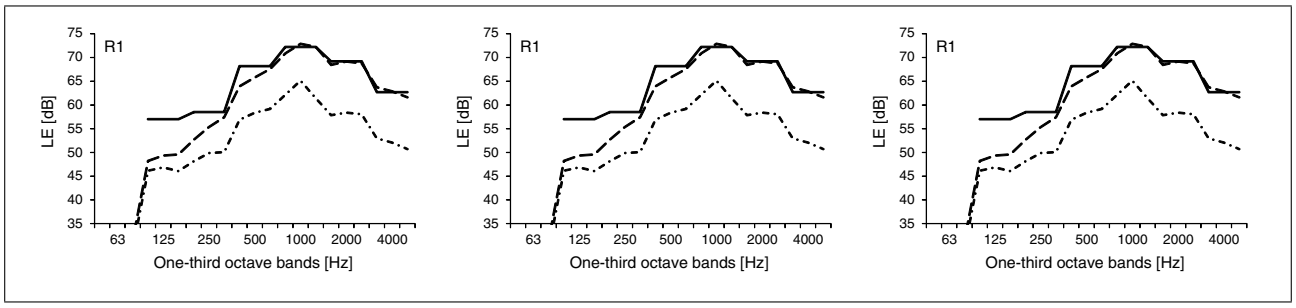


Figure 10. Measured sound exposure spectra of forest reflections 'Dinhard' 1993 (solid line) compared to model calculations (dashed line). Additionally, calculations with only contributions from the tree trunks are shown as dash-dotted lines.

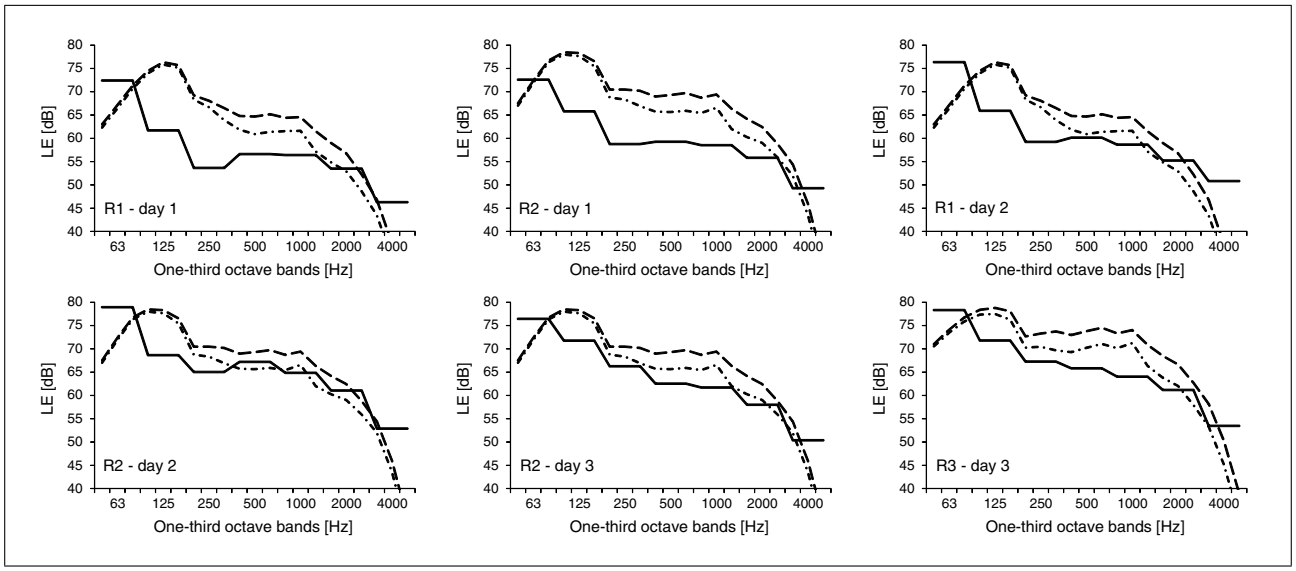


Figure 11. Measured sound exposure spectra of forest reflections 'Thun' 2002 (solid line) compared to model calculations (dashed line). Additionally, calculations with only contributions from the tree trunks are shown as dash-dotted lines.

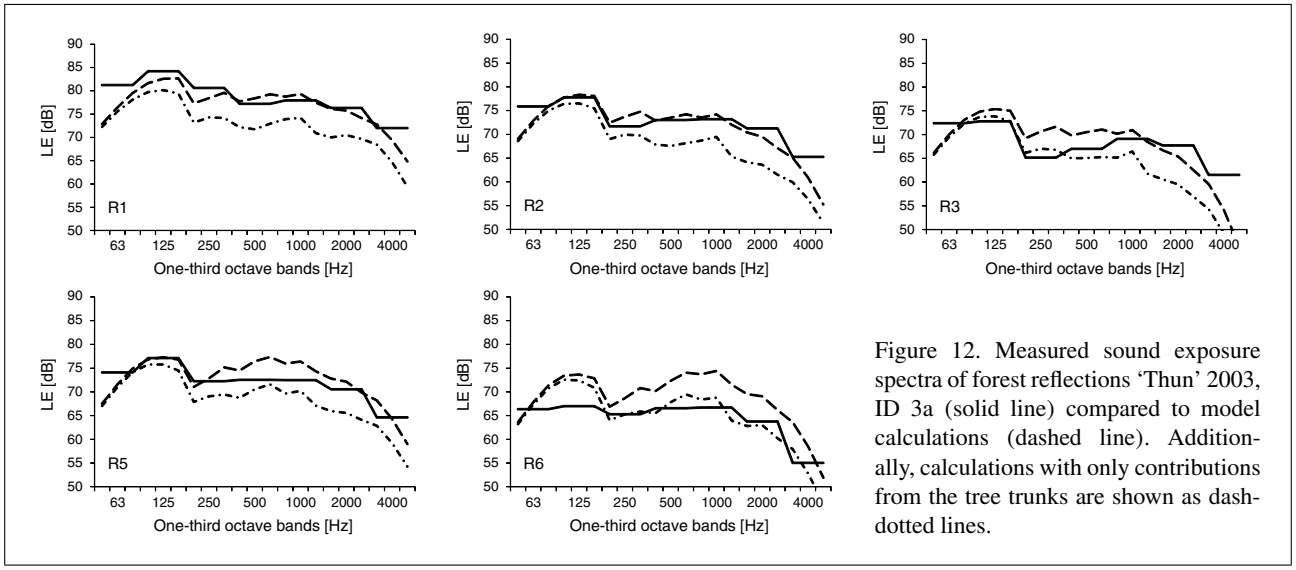


Figure 12. Measured sound exposure spectra of forest reflections 'Thun' 2003, ID 3a (solid line) compared to model calculations (dashed line). Additionally, calculations with only contributions from the tree trunks are shown as dash-dotted lines.

between 50 and 300 m from the forest edge. For most source-receiver-combinations the propagation distances were smaller than in 2002. However some combinations even exhibited greater propagation distances. As can be seen in Figures 12 to 15 the agreement between measurement and calculations is rather good with 80% of all deviations smaller than ± 4.5 dB in 2003 and 65% in 2007. Greater deviations in the spectral characteristics are on the one hand visible around 200 Hz, where in some situations a prominent ground dip is visible, and on the other hand

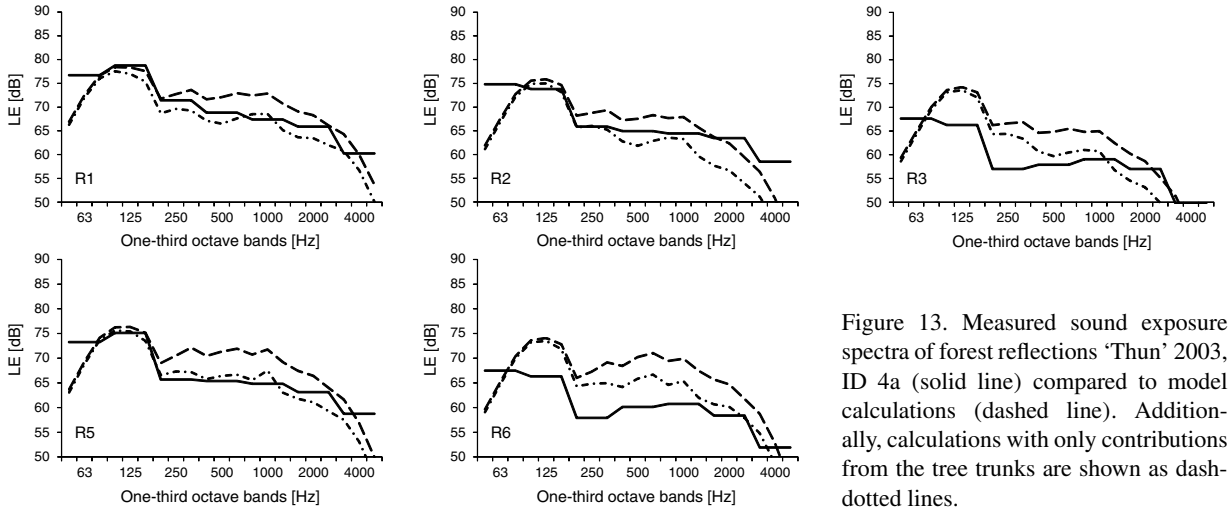


Figure 13. Measured sound exposure spectra of forest reflections 'Thun' 2003, ID 4a (solid line) compared to model calculations (dashed line). Additionally, calculations with only contributions from the tree trunks are shown as dash-dotted lines.

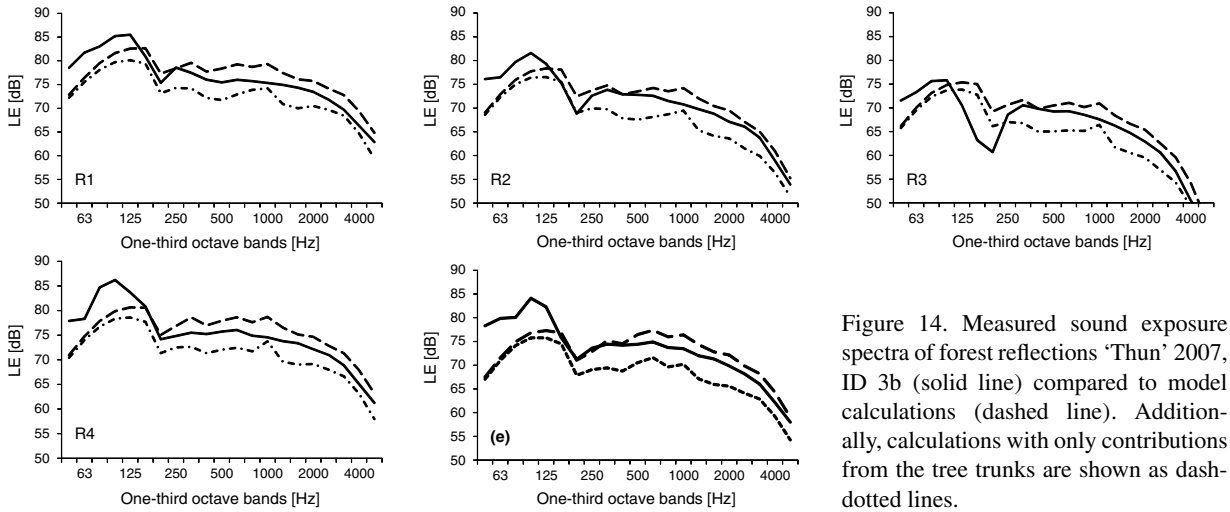


Figure 14. Measured sound exposure spectra of forest reflections 'Thun' 2007, ID 3b (solid line) compared to model calculations (dashed line). Additionally, calculations with only contributions from the tree trunks are shown as dash-dotted lines.

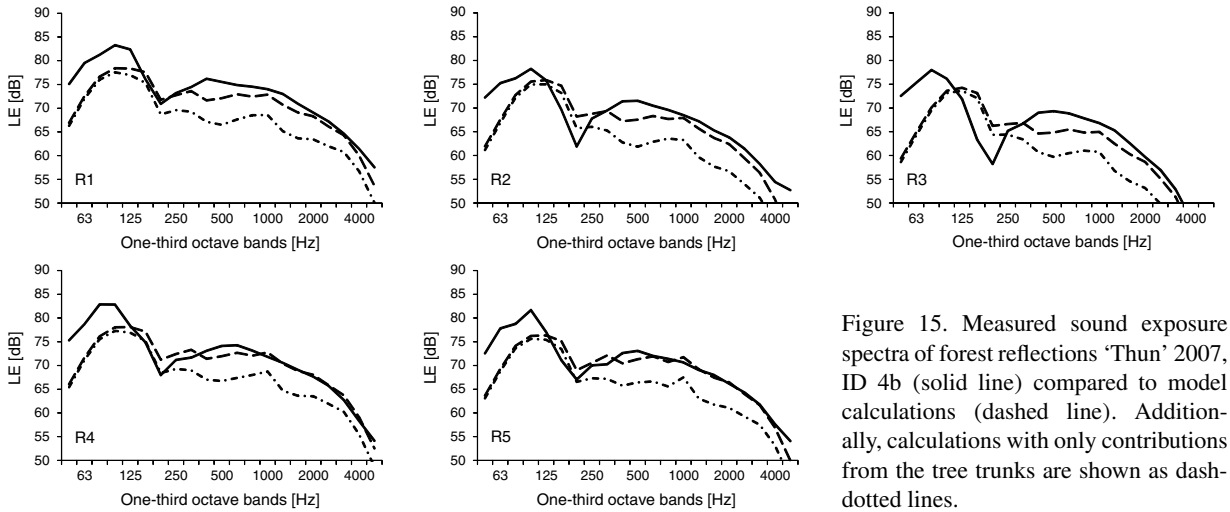


Figure 15. Measured sound exposure spectra of forest reflections 'Thun' 2007, ID 4b (solid line) compared to model calculations (dashed line). Additionally, calculations with only contributions from the tree trunks are shown as dash-dotted lines.

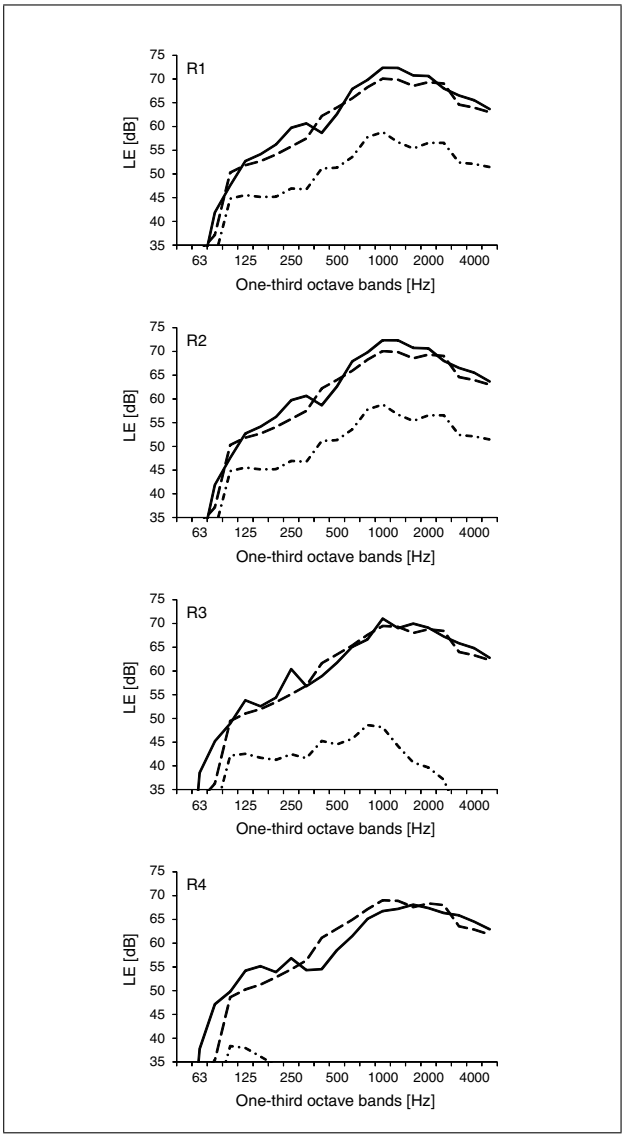


Figure 16. Measured sound exposure spectra of forest reflections 'Eglisau' 2009, ID 5a (solid line) compared to model calculations (dashed line). Calculations with only contributions from the tree trunks are visible in some graphs as dash-dotted lines. In the other graphs the contributions from the tree trunks are not visible anymore as a consequence of the steep vertical reflection angle.

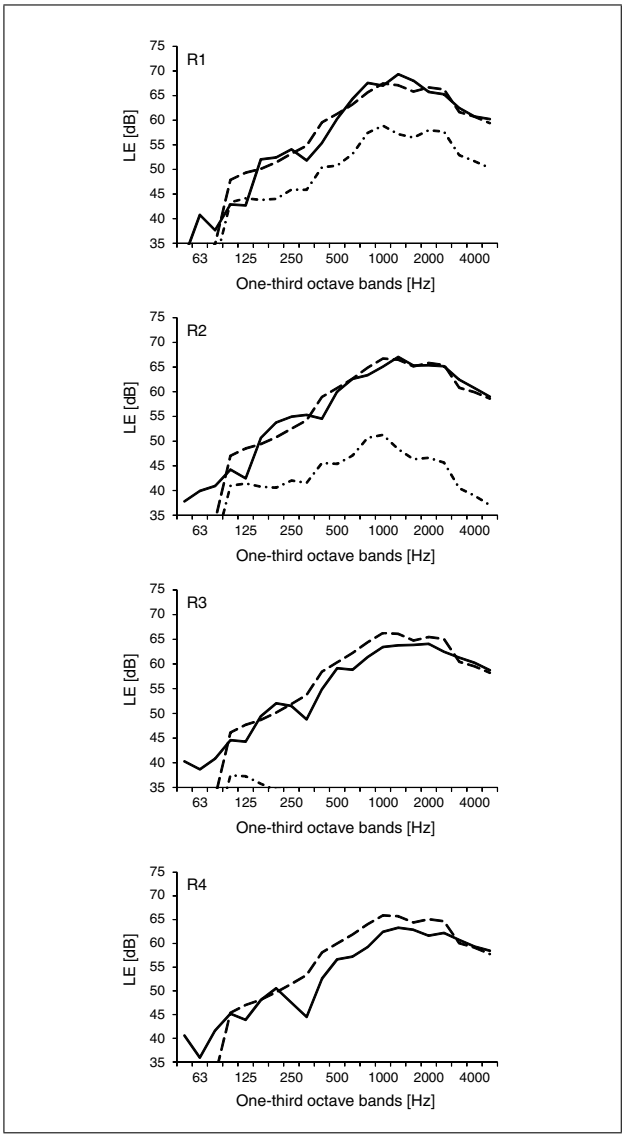


Figure 17. Measured sound exposure spectra of forest reflections 'Eglisau' 2009, ID 5b (solid line) compared to model calculations (dashed line). Calculations with only contributions from the tree trunks are visible in some graphs as dash-dotted lines. In the other graphs the contributions from the tree trunks are not visible anymore as a consequence of the steep vertical reflection angle.

below 100 Hz, where measurements exhibit a tendency to higher level than calculations.

The measurement data of 'Eglisau' is generally very well reproduced by calculations with 79% of all one-third octave band deviations lying within ± 4.5 dB. Despite the similar geometry the accordance in 'Wald' is worse with only 50% of the deviations within ± 4.5 dB. While in 'Eglisau' the measurements are reproduced very well in average, the measured sound exposure levels in 'Wald' are systematically underestimated by calculations, i.e., in 92% of all cases. These much stronger reflections in 'Wald' than in 'Eglisau' can be explained by the peculiarities of the two forests involved. While the forest measured in 'Eglisau' consisted of hardwood with only a few branches in great height and tree diameters below average, the trees in 'Wald' were old softwood trees with mighty trunks and branches, that almost touched the ground.

Additionally Figure 26 shows a compilation of all cases, where A-weighted attenuations are compared. The average deviation between measurements and calculations is -0.1 dB(A), the standard deviation amounts to 3.4 dB(A). While the average deviation is very small as the model parameters for the number of reflecting spheres N_{sph} and the weighting of the cylinder contribution w_{cyl} have been fitted on the basis of this dataset, the standard deviation can be taken as an assessment of the model accuracy. Major deviations are on the one hand visible in situations with greater propagation distances and therefore greater attenu-

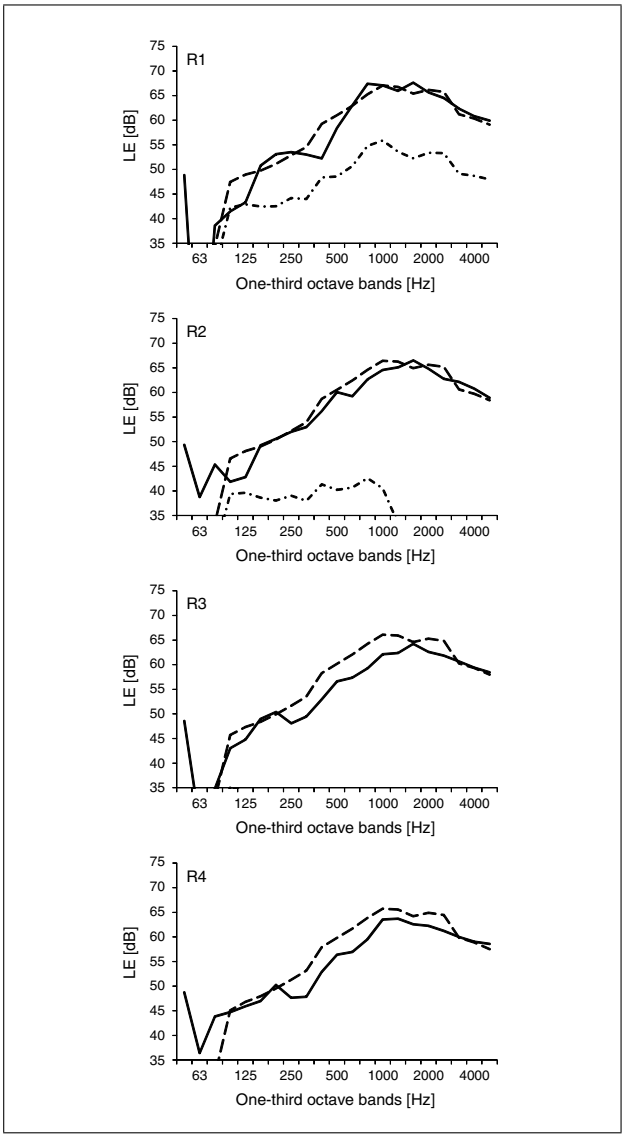


Figure 18. Measured sound exposure spectra of forest reflections 'Eglisau' 2009, ID 5c (solid line) compared to model calculations (dashed line). In the uppermost graph to the left calculations with only contributions from the tree trunks are shown as dash-dotted lines. In the other graphs the contributions from the tree trunks are not visible anymore as a consequence of the steep vertical reflection angle.

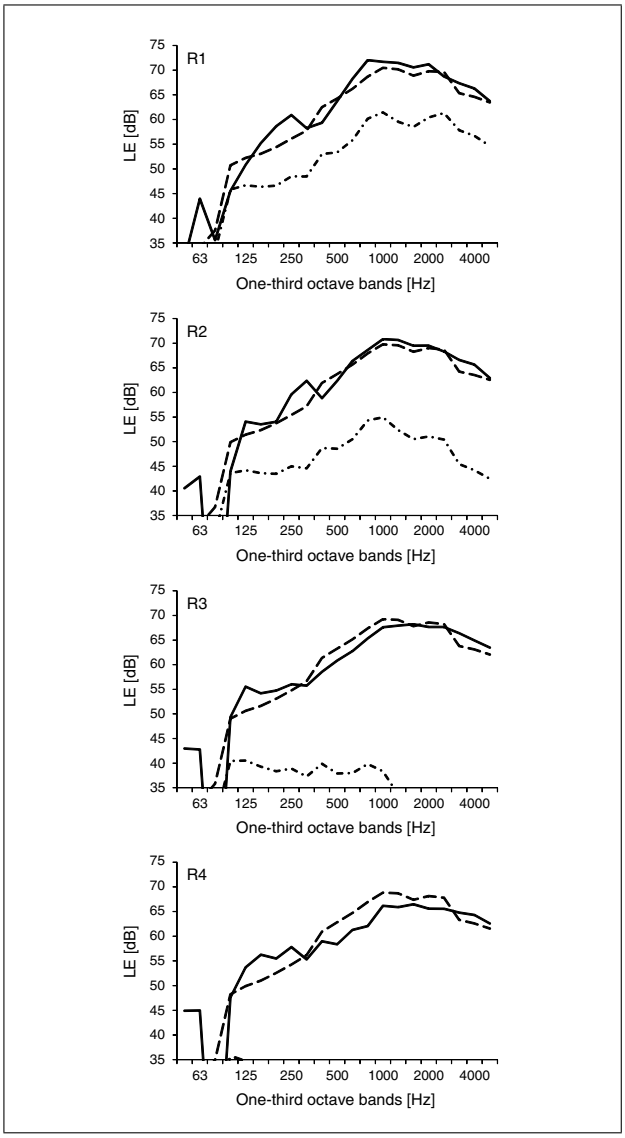


Figure 19. Measured sound exposure spectra of forest reflections 'Eglisau' 2009, ID 5d (solid line) compared to model calculations (dashed line). Calculations with only contributions from the tree trunks are not visible anymore as a consequence of the steep vertical reflection angle.

ations. Overlayed to this is a general range of uncertainty as a consequence of the individual attributes of the forests. This becomes especially clear when comparing the data from 'Eglisau' and 'Wald' that exhibit on the one hand differing overall level of reflection and on the other hand also a diverse vertical directivity pattern, the latter being much more prominent in 'Eglisau' as a consequence of the smaller contributions from branches.

5. Discussion

The presented calculation model for forest reflections is based on a model that was published in 2009 [1]. The parent model represented a single tree only by its trunk. As can be seen in Figures 11 to 15 the correspondent cylinder reflections reproduce the measured values quite accurately as long as the propagation distance amounts to several hundred meters. However close to the forest edge pure cylinder reflections underestimate the resulting sound exposure levels significantly (see Figures 10 and 18 to 24). Here the model extension that aims at representing reflections from the branches produces a major improvement of the model accuracy. Additionally with the implementation of a Fresnel-zone-approach for the cylinder reflections, the influence of the tree height as well as the vertical directivity of forest reflections can be reproduced, which allows a model application also in non-flat situations.

The extended forest reflection model has been validated in comparison with extensive measurements. The validation has on purpose been performed on the basis of a simplified implementation of the model and with standard val-

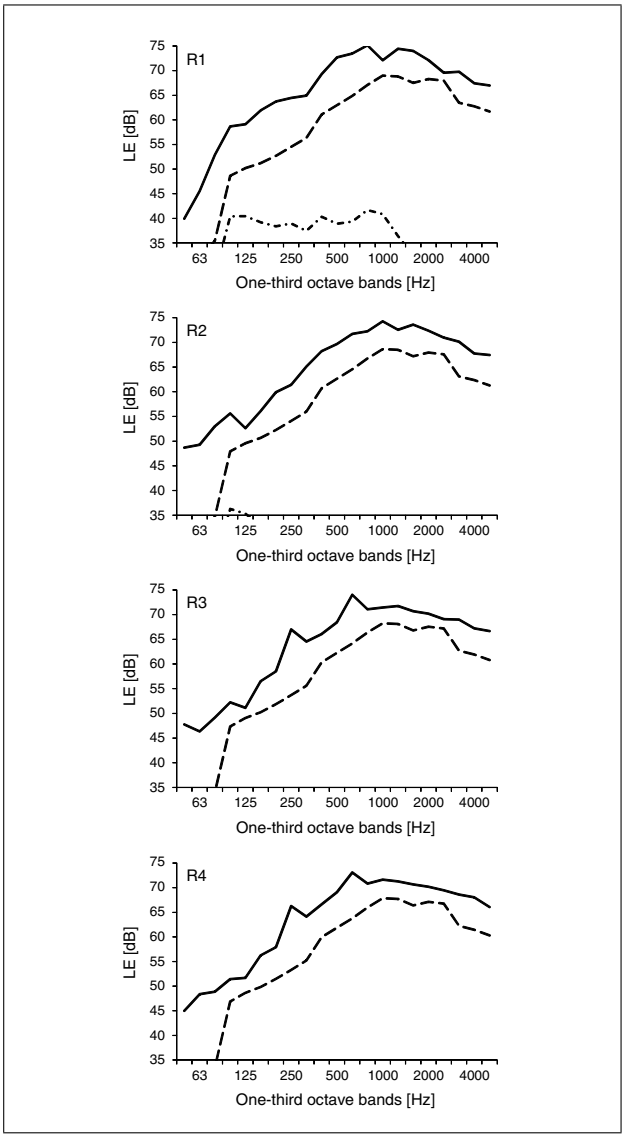


Figure 20. Measured sound exposure spectra of forest reflections 'Wald' 2009, ID 6e (solid line) compared to model calculations (dashed line). Calculations with only contributions from the tree trunks are not visible anymore as a consequence of the steep vertical reflection angle.

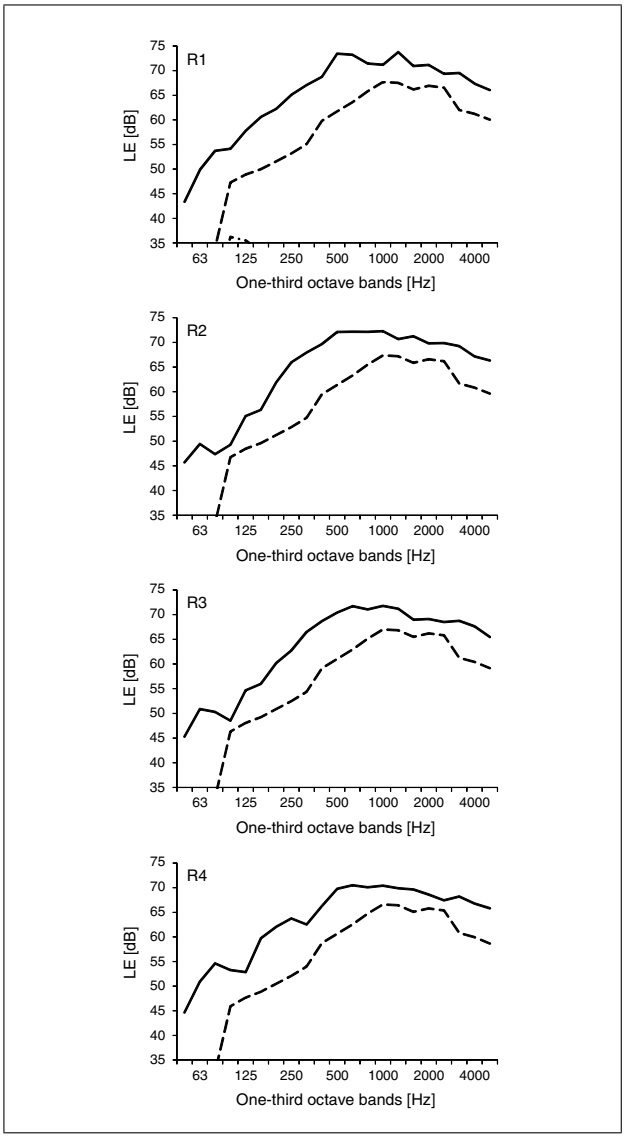


Figure 21. Measured sound exposure spectra of forest reflections 'Wald' 2009, ID 6b (solid line) compared to model calculations (dashed line). In the uppermost graph to the left calculations with only contributions from the tree trunks are shown as dotted lines. In the other graphs the contributions from the tree trunks are not visible anymore as a consequence of the steep vertical reflection angle.

ues for the forest properties to give an accurate estimate of the models capacity under conditions which are representative for noise mapping. For propagation distances smaller than 500 m the agreement between measurement and calculation is generally good with a standard deviation of 2.9 dB(A). However for greater propagation distances the measurements indicate a systematic overestimation of the resulting sound exposure level. Two possible causes have been identified. On the one hand certainly meteorological effects on sound propagation become relevant at such propagation distances. According influences are visible in the measured data of 'Thun'. The measurements performed in the year 2002 exhibited deviations of 3 to 6 dB(A) at the same microphone positions but at different days of measurement. Additionally when looking at the meteorological data, it must be concluded that conditions were primarily adverse for sound propagation from source to receiver at all days, either because of the dominating wind direction or as a consequence of the strong incoming radiation. Only in 2007 downwind conditions were measured. In comparison with the data of 2003, that was gathered at the same source and receiver positions but with upwind conditions, an average difference of the reflected sound exposure level of 3.4 dB(A) resulted with up to 7 dB(A) at most.

A second potential cause for the systematic overestimation at greater propagation distances might be found in the peculiarity of a reflection at a cylinder of 20 m height. The analytical solution for the cylinder reflection that is used in the model is based on the assumption of an undisturbed

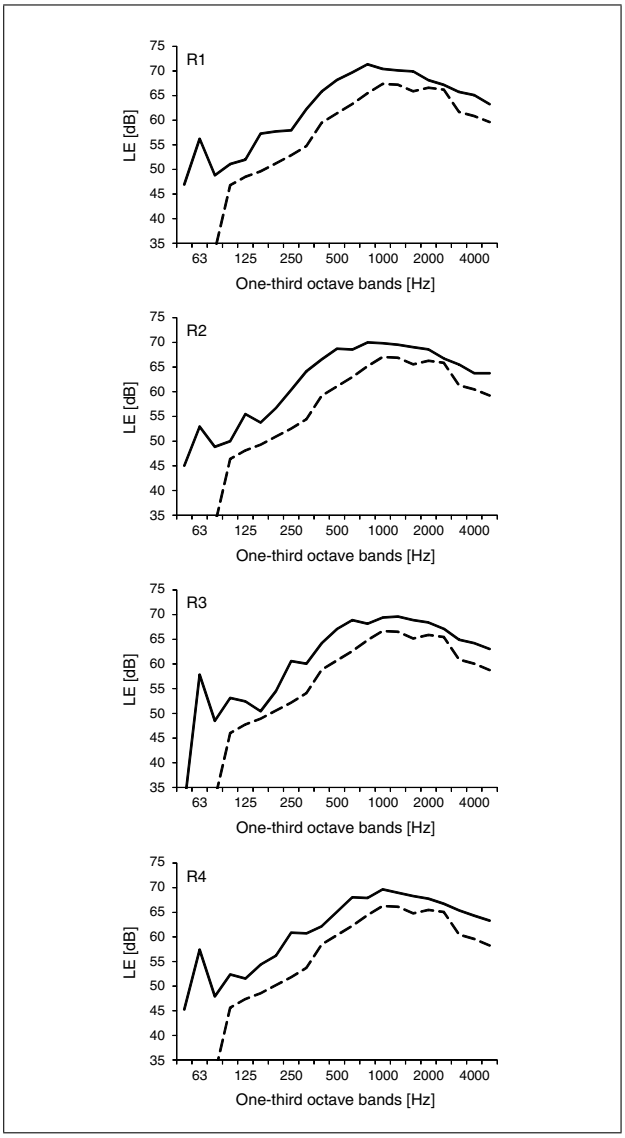


Figure 22. Measured sound exposure spectra of forest reflections 'Wald' 2009, ID 6c (solid line) compared to model calculations (dashed line). Calculations with only contributions from the tree trunks are not visible anymore as a consequence of the steep vertical reflection angle.

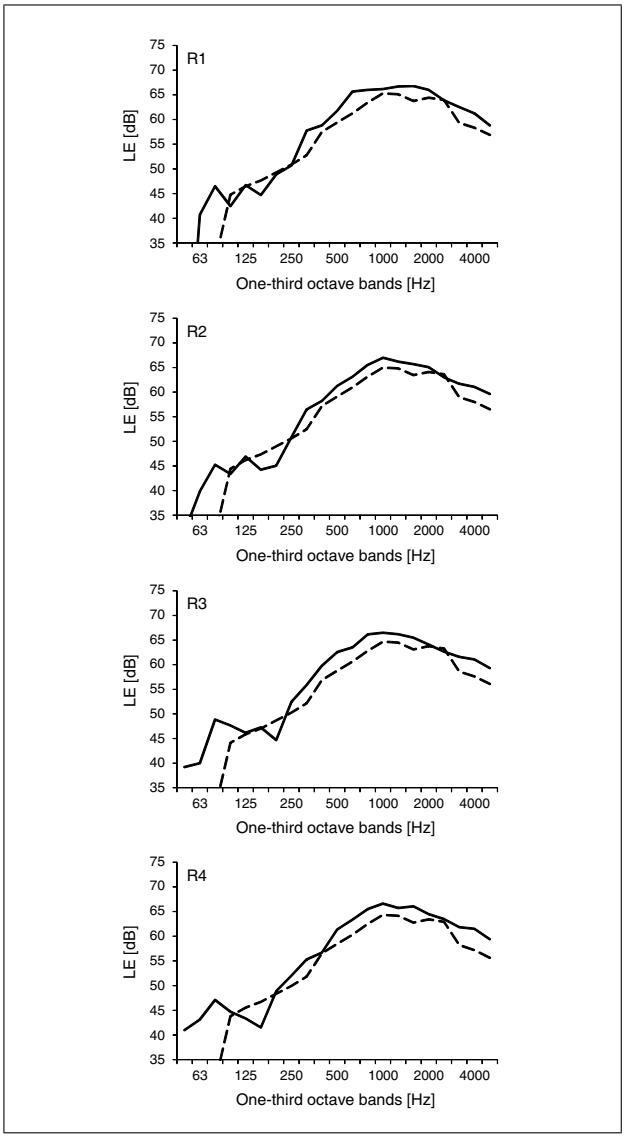


Figure 23. Measured sound exposure spectra of forest reflections 'Wald' 2009, ID 6d (solid line) compared to model calculations (dashed line). Calculations with only contributions from the tree trunks are not visible anymore as a consequence of the steep vertical reflection angle.

phase-relation of all contributions. Yet the sound propagation paths of reflections from the root point differ significantly of those from the treetop. Under the influence of turbulence and differing effective sound speeds the phase relation is likely to get disturbed. The greater the propagation distance the more pronounced is the loss of phase relation and the higher are the frequencies that need the entire cylinder for a full reflection.

Up to propagation distances of 500 m the forest properties can be identified as the major source of uncertainty. The cylinder reflections are primarily influenced by the number of trees per area and the average cylinder diameter. An influencing parameter of second order is the average tree height. On the basis of statistical data about properties of different forest types of Switzerland published in [1] the standard deviation of the contribution from the trunks is deduced to be in the orderof 1–2 dB(A). The contribution from the canopy is subjected to greater deviations as the number, position and thickness of the branches can vary much more than the trunk diameter. In this respect no statistical data is available. However when comparing the measurements of 'Eglisau' and 'Wald', which were performed on forest edges with hardly any and very prominent branches, the influence on the resulting sound exposure can be estimated to be in the order of 3 dB(A). To get a greater accuracy of the model for a distinct forest type or to apply the model in a climate zone that differs systematically from the conditions in Switzerland, representative values of the free model parameters have to be identified. The average tree diameter and height as well as the forest density are directly represented as parameters. The relevance of the canopy reflection, which is mainly

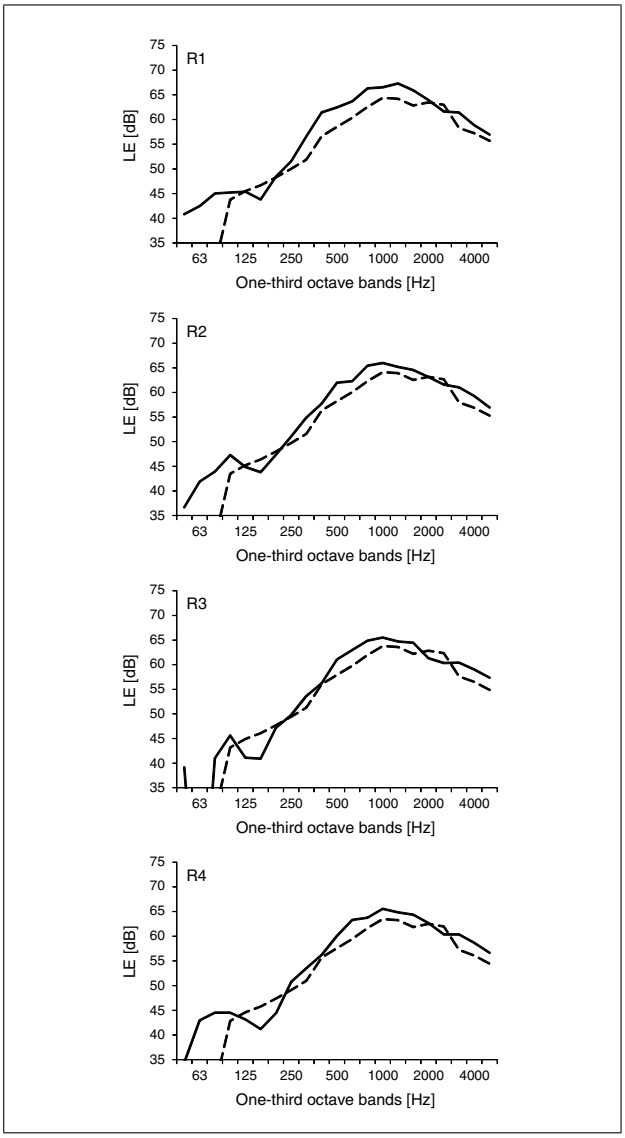


Figure 24. Measured sound exposure spectra of forest reflections 'Wald' 2009, ID 6e (solid line) compared to model calculations (dashed line). Calculations with only contributions from the tree trunks are not visible anymore as a consequence of the steep vertical reflection angle.

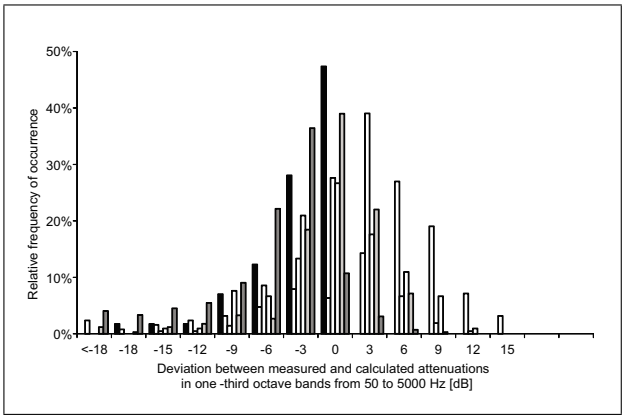


Figure 25. Frequency of occurrence of deviations between measured and calculated forest reflection attenuations in one-third octave bands from 50 to 5000 Hz for all cases. The attenuation is defined as the difference of the sound energy level according to Figure 9 and the measured or calculated sound exposure level in one-third octave bands. The classwidth is 3 dB. The classes are designated with the class averages.

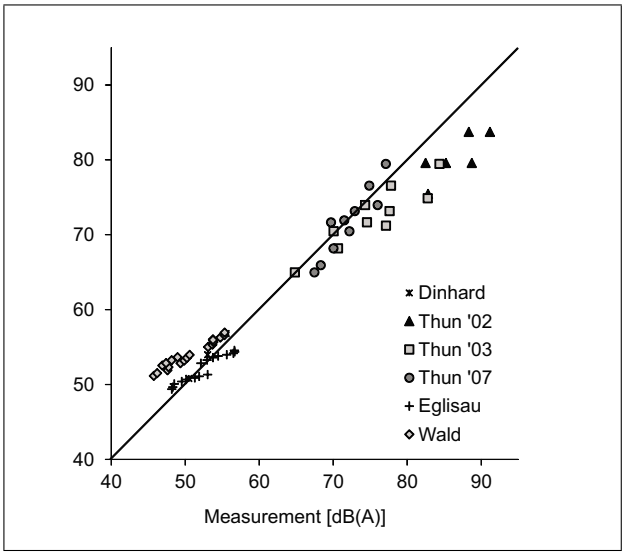


Figure 26. Measured vs. calculated attenuations in dB(A) of forest reflections for all cases. The attenuation is defined as the difference of the A-weighted sound energy level according to Figure 9 and the measured or calculated sound exposure level.

defined by the type of trees (hardwood or softwood), has to be regulated through the number of spheres N_{sph}, set to 250. Looking at the average underestimation of about 3 dB(A) in 'Wald', a value of 500 would for example be an appropriate choice for forests with pure softwood.

Apart from using specific forest properties the model accuracy could certainly be raised by improving the sound propagation calculation. Instead of relying on the simplified approach presented in section 3 a propagation calculation could be performed for every propagation path to each tree individually with a sophisticated propagation model, which is also able to take meteorological effects into account. However the assessment of meteorological influences on forest reflection is challenging, on the one hand as the propagation path is not following a single direction and on the other hand as the presence of the forest itself influences wind fields as well as the temperature stratification [11], [16], [17]. Generally it has to be questioned though whether it is appropriate to increase the expense for such calculations, both in the modeling process as well as in the data acquisition. Taking forest reflections into account is primarily a refinement of direct sound calculations. Therefore the calculation effort should be kept low compared to the prediction of direct sound. Having to deal with a great number of reflectors this can only be achieved by major simplifications in the propagation calculation. Hence it can be concluded that the model presented here exhibits a good compromise between accuracy and calculation costs and is suitable for the implementation in engineering sound propagation models.

Acknowledgment

This work was supported by the Defence Procurement Agency of Switzerland (armasuisse) and the Federal Office for the Environment of Switzerland (FOEN).

References

[1] J. M. Wunderli, E. M. Salomons: A model to predict the sound reflection from forests. Acta Acustica United with Acustica **95** (2009) 76–85.

[2] D. Sehu, J. M. Wunderli, K. Heutschi, T. Thron, M. Hecht, A. Rohrbeck, T. Ledermann: "Sonrail - Projektdokumentation". PDF Bundesamt fuer Umwelt (Bafu), 2010. http://www.bafu.admin.ch/laerm/10312/10313/10318/10320/index.html?lang=de.

[3] R. Pieren, J. M. Wunderli: A model to predict sound reflections from cliffs. Acta Acustica United with Acustica **97** (2011) 243–253.

[4] P. Morse, K. Ingard: Theoretical acoustics. McGraw-Hill, New York (1968).

[5] International Organization of Standardization: Iso 9613-1: Acoustics - Attenuation of sound during propagation outdoors. Part 1: Calculation of the absorption of sound by the atmosphere. 1993.

[6] International Organization of Standardization: Iso 9613-2: Acoustics - Attenuation of sound during propagation outdoors. Part 2: General method of calculation. 1996.

[7] R. Blumrich, D. Heimann: A linearized Eulerian sound propagation model for studies of complex meteorological effects. Journal of the Acoustical Society of America **112** (2002) 446–455.

[8] E. Salomons: Computational atmospheric acoustics. Kluwer, Dordrecht (2001).

[9] M. A. Price, K. Attenborough, N. W. Heap: Sound-attenuation through trees - measurements and models. Journal of the Acoustical Society of America **84** (1988) 1836–1844.

[10] W. H. T. Huisman, K. Attenborough: Reverberation and attenuation in a pine forest. Journal of the Acoustical Society of America **90** (1991) 2664–2677.

[11] M. Ringheim: Attenuation of sound through vegetation: Some results from a literature survey. Proceedings of the workshop on sound propagation in forested areas and shelterbelts, M. Martens (ed.), 13–24.

[12] L. Cremer: Fresnels Methoden zur Berechnung von Beugungsfeldern. Acustica **72** (1990) 1 – 6.

[13] International Organization of Standardization: Iso 17201-2: Acoustics - Noise from shooting ranges. Part 2: Estimation of muzzle blast and projectile sound by calculation. 2006.

[14] International Organization of Standardization: Iso 13474: Acoustics - Framework for calculating a distribution of sound exposure levels of impulsive sound events for the purposes of environmental noise assessment. 2001.

[15] J. M. Wunderli: Modelling the source strength of explosions under consideration of the ground influence. Acta Acustica United with Acustica **90** (2004) 690–701.

[16] D. Heimann: Numerical simulations of wind and sound propagation through an idealised stand of trees. Acta Acustica United with Acustica **89** (2003) 779–788.

[17] M. E. Swearingen, M. J. White: Influence of scattering, atmospheric refraction, and ground effect on sound propagation through a pine forest. Journal of the Acoustical Society of America **122** (2007) 113–119.